Journal of ELECTRONIC MATERIALS, Vol. 45, No. 10, 2016
DOI: 10.1007/s11664-016-4712-1

Method and Apparatus for Determining Operational Parameters of Thermoelectric Modules

RAFAŁ ZYBAŁA,[1,3] MAKSYMILIAN SCHMIDT,[2] KAMIL KASZYCA,[2] ŁUKASZ CIUPIŃSKI,[1] MIROSŁAW J. KRUSZEWSKI,[1] and KATARZYNA PIETRZAK[2]

1.—WUT Warsaw University of Technology, Wołoska 141, 02-507 Warsaw, Poland. 2.—ITME Institute of Electronic Materials Technology, Wólczyńska 133, 01-919 Warsaw, Poland. 3.—e-mail: rafal.zybala@inmat.pw.edu.pl

The main aim of this work was to construct and test an apparatus for characterization of high temperature thermoelectric modules to be used in thermoelectric generator (TEGs) applications. The idea of this apparatus is based on very precise measurements of heat fluxes passing through the thermoelectric (TE) module, at both its hot and cold sides. The electrical properties of the module, under different temperature and load conditions, were used to estimate efficiency of energy conversion based on electrical and thermal energy conservation analysis. The temperature of the cold side, T_c, was stabilized by a precise circulating thermostat (≤0.1°C) in a temperature range from 5°C to 90°C. The amount of heat absorbed by a coolant flowing through the heat sink was measured by the calibrated and certified heat flow meter with an accuracy better than 1%. The temperature of the hot side, T_h, was forced to assumed temperature (T_{max} = 450°C) by an electric heater with known power (P_h = 0–600 W) with ample thermal insulation. The electrical power was used in calculations. The TE module, heaters and cooling plate were placed in an adiabatic vacuum chamber. The load characteristics of the module were evaluated using an electronically controlled current source as a load. The apparatus may be used to determine the essential parameters of TE modules (open circuit voltage, U_{oc}, short circuit current, I_{sc}, internal electrical resistance, R_{int}, thermal resistance, R_{th}, power density, and efficiency, η, as a function of T_c and T_h). Several commercially available TE modules based on Bi_2Te_3 and Sb_2Te_3 alloys were tested. The measurements confirmed that the constructed apparatus was highly accurate, stable and yielded reproducible results; therefore, it is a reliable tool for the development of thermoelectric generators.

Key words: Energy conversion efficiency, power generation, thermoelectric modules, performance characterization, heat recovery, renewable energy

INTRODUCTION

Direct energy conversion from heat into electricity takes place in thermoelectric generators (TEGs) made from coupled *n*- and *p*-type carrier thermoelectric material (unicouple) by way of the Seebeck effect. The energy conversion efficiency is closely related to the Carnot cycle efficiency and material properties expressed by thermoelectric figure-of-merit (ZT).[1] Because the voltage of one unicouple is very small, TEGs have to be constructed of a number of such pairs connected electrically in series and thermally in parallel.[2] As a result, TEG efficiency depends on many factors such as design issues, including dimensions of the modules and

(Received February 15, 2016; accepted May 27, 2016; published online June 23, 2016)

number of the unicouples, material parameters (ZT, electrical and thermal contact resistance, properties of insulation plates), and operating conditions (temperature range, load parameters). Therefore a number of parameters can limit the TEG performance, and the best way to compare thermoelectric modules is based on measurement of their efficiency of energy conversion.

The aspects of measuring parameters of thermoelectric modules have not been described thoroughly. The efficiency is often estimated from functional thermoelectric material properties as well as those of auxiliary materials (metallic interconnectors, ceramic plates, protective covers, etc.). However, recently an interest in the real TEG operating parameters is stimulated, because of possibility of a wide range of home and industrial applications.[1–4] The performance evaluation of the modules, and a precise characterisation of their operational parameters became a necessary requirement.[2,3]

The most popular thermoelectric modules (also evaluated in this work) are based on bismuth telluride alloys.[5–8] Because this widely used material possesses a moderate value of ZT ($ZT = 1$), current research concentrates on modifications of its composition and structure in nano- and microscale[1,5–10] aimed at improving ZT. Concurrently, there is constant progress in the optimization of other TE materials.[1,2,10–13] Meanwhile, other critical developments in the module construction, such as in the area of materials junctions (ceramic–metal-TE material, barriers and bonders), are ongoing,[14–16] including quality measurements of thermoelectric—thermoelectric (TE–TE) junction in cascaded modules.[17,18] The lifetime and the reliability of thermoelectric modules are also important.[19] Another aspect is materials that could provide heat transport from the heat source and to the heat sink.[20] All these efforts should enable the development of TEGs with improved efficiency of energy conversion and possibilities of application in everyday life.[21] This inevitably leads to the next step, which is precise measurements of their performance before widespread applications.

The general idea of efficiency measurements, applied in this study, is based on comparison of electrical power, P_{el}, generated by the module and the thermal power, Q_1^*, supplied to the hot side of the module in stationary heat flow conditions, and Q_2^* heat received from the cooler. Measurements of electrical parameters (output voltage, U_{out}, and current, I_{out}) and electrical power, P_{el}, are quite simple and very accurate. In contrast, it is a challenge to achieve a precise measurement of the heat flow supplied to the TE module and measuring all temperatures in the system. Takazawa et al.[22] constructed an apparatus designed to examine modules operating in temperature differences of up to 550°C. The technique was based on the concept of thermal conductivity measurements using a stationary comparative method in adiabatic conditions. In this technique, temperatures are measured in aluminium nitride (AlN) plates in contact with module and heater (contact provided by carbon sheet). The amount of heat flow at the cold side of the module was estimated by measuring the difference in temperature in a Cu block (temperature calibrated by the standard reference material Fe), mounted on the cold side of the thermoelectric module. As in the case of the stationary comparative method for measuring the thermal conductivity, the main difficulty in precise measurements is due to heat radiation losses in the reference materials and uncertainty in temperature measurements, which cause systematic errors in values of the heat flow and consequently in estimated parameters. Therefore, during Takazawa's efficiency measurements, the temperature of the Cu block was maintained around $T_c = 25$°C in the cold stage. The phenomenon of heat losses in the Cu block (heat flow sensor) limits the practical temperature range of the apparatus usage to cold side temperatures, T_c, of about 20–60°C. The measured deviation of the heat flux parameters was lower than ±5%. A similar solution was presented in a study[23] where two reference blocks were applied on both sides of the measured modules. The temperature range of the hot side was up to 580°C and the cold side, $T_c = 30$°C. The authors estimated again the error as ±5%.

In order to overcome the high degree of uncertainty involved in measuring heat flow using the absolute method, Rauscher et al.[24] proposed a different solution. In their concept, amounts of heat were measured based on the power dissipation of the thermally guarded electrical heater that supplied the thermal energy to the hot side of the module. The heat flow measurements for a reference sample were reliable within ±5%. The estimated systematic error of the heat flux and the efficiency were within 3%. Similar studies and methods can be found in papers concerning measurements of thermoelectric generator parameters.[25] In Ref. 26 the heat flux was measured at the cold side of the module by a heat meter (reference material and thermocouples) and concurrently by the heat meter mounted on a cooling system (with liquid coolant). At the hot side, the same heat meter was used for proportional-integral-derivative (PID) controller application, in which case determination of electric power of the heater was hindered. Nevertheless the heat flux errors, as claimed by the authors, did not exceed 3% for this setup. The electric current measurements were carried out on an analogue resistor that should not introduce measurement errors according to the authors. The overall estimated error of efficiencies did not exceed 3%. A similar apparatus has been presented,[27] but that work additionally introduced an analytical model to analyse the impact of the modules' most important properties and thermal interface leakage on the

measured efficiency. The authors of[28] analyse different internal heat loss mechanisms for thermoelectric generators with Bi_2Te_3 *p*- and *n*-type legs. They did not consider heat losses through the sides of the module. The heat losses due to natural convection were negligible for millimetre size module. The combined case of radiative and conductive heat transfer resulted in the lowest efficiency. For an insulator with properties similar to argon, only the radiative path was responsible for significant heat losses. The overall efficiency was decreased by the inner heat losses (for distance between legs equal to 1 mm and temperatures, T_c = 20°C and T_h = 250°C) by less than 3% of the absolute value.

This introduction indicates that there is need to make an effort to evolve and construct a new apparatus for measuring TE modules, one able to describe the operating properties of the module with better precision.

The concept, design and construction of an apparatus for measuring the thermoelectric modules for high temperature applications are presented here, along with results of measurements carried out for commercially available modules. The apparatus has been used also during a study devoted to development of segmented $Bi_2Te_3/CoSb_3$, for which the results were presented at the 9th European Conference on Thermoelectrics (ECT).[29] The technical details of the apparatus construction can be found in Ref. 30.

OPERATING PARAMETERS AND THE CONCEPT OF THE APPARATUS

The apparatus operating temperature ranges are T_h = 30–450°C at the hot side, and T_c = 5–90°C at the cold side. These temperatures can be adjusted, so that module parameters can be measured in their respective maximum temperature ranges and at the same time to avoid the module thermal destruction.

In particular, the equipment can be used to determine the following essential parameters of thermoelectric modules:

- Open circuit voltage U_{oc} as a function of temperature, both of T_h and T_c
- Short circuit current I_{sc} as a function of temperature, both T_h and T_c
- Internal electrical resistance R_{int} as a function of temperature
- Current–voltage characteristics, *U-f(I)*
- Thermal resistivity as a temperature function, R_{th}
- Energy conversion efficiency, η
- Thermoelectric figure of merit, *ZT*
- Power density

The general underlying concept of the measuring method is presented in Fig. 1. The apparatus components are placed in a vacuum chamber and covered by insulation. The chamber can be filled

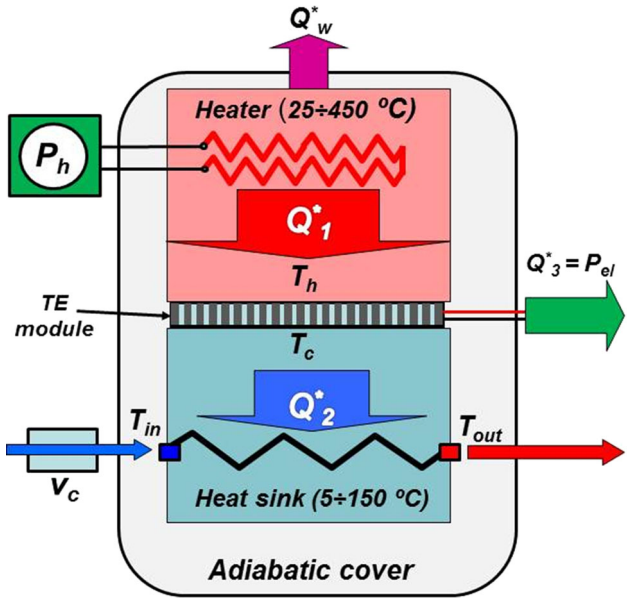

Fig. 1. The idea behind the method of measuring thermoelectric modules.

by inert gasses (Ar, N_2) or evacuated to a vacuum of 10^{-3} bar. The module is placed between heater with hot temperature, T_h, (hot side of the module) and cooler with cold temperature, T_c (cold side of the module). A controlled electrical supply provides energy to the heater, P_h. When we increased the current output during measurement, the system adjusts the heater power to maintain the same hot side temperature. The heat energy that does not reach the TE module is described by Q^*_w. The thermal power provided to the thermoelectric element Q^*_1 is calculated from Q^*_2 and P_{el}, where the thermal power absorbed by cooler is Q^*_2, and P_{el} is electrical power generated by the thermoelectric module. For Q^*_2 calculation, one needs to know additional cooling medium parameters, that is, T_{in} and T_{out} (the coolant temperature at the input and output of the cooler), the coolant flow rate, v_c, and thermal capacity of the coolant, c_p.

Figure 2 shows a schematic diagram of the constructed apparatus. The thermoelectric module is placed between the source of heat (electric heater) and the heat sink (with liquid coolant). In order to ensure a precise determination of the energy balance, both the heat flux entering the thermoelectric module Q^*_1 and the heat flux absorbed by the heat sink Q^*_2 are measured. The apparatus includes a power supply and a heater with power regulator, P_h = 0–600 W, and an active load source with adjustable current, $I = \pm$ 0…30 A. The central control unit provides control and acquisition of all parameters. The cooling system is composed of heat exchanger, pump, and ultrasonic flow meter with two temperature sensors (T_{in}, T_{out}). The vacuum chamber is connected to a vacuum pump. The

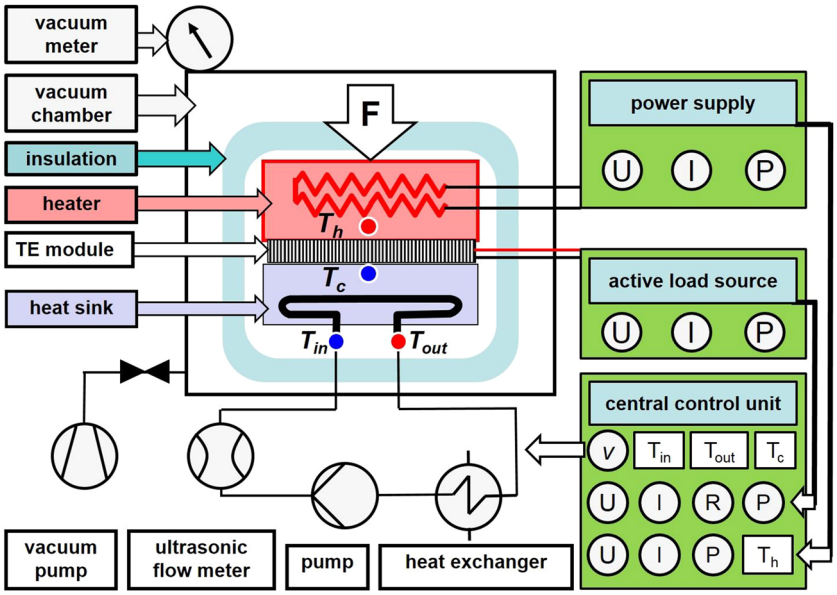

Fig. 2. Schematic diagram of constructed apparatus.

heater, TE module, and heat sink were all insulated.

ENERGY BALANCE AND EFFICIENCY OF THE TE MODULE

The apparatus is constructed in a way that provides precise heat and electrical measurements. Collected data from the electrical measurements are used for the calculations of the electrical power of the TE module. The electrical and heat quantities from the measurements are used for energy conversion efficiency calculations. The amount of heat passing through the heat sink for varied current flow is used to estimate the Peltier coefficient. The Joule and Peltier heat are calculated from the electrical current. The idea of the calculations is described below.

The heat flux supplied by the heater to the TE module Q_1^* is:

$$Q_1^* = P_h - Q_w^* \tag{1}$$

where P_h is the electric power of the heater ($P_\mathrm{h} = I_\mathrm{h} \cdot \mathrm{U_h}$) and Q_w^* is the amount of heat losses dissipated to the environment by radiation and convection on the hot side of the module.

Energy losses inside the module through radiation, conduction and convection are described in Ref. 28 and are similar to those in our case, because the material and temperature ranges are comparable, thus, those losses reduce maximum efficiency by about 3% (for $T_\mathrm{h} = T_\mathrm{max}$).

However, the energy losses from the heater are different for our case. In our experiment, Q_w^* was equal to about 30% of P_h, but we did not use this value to calculate Q_1^*. Our methods for calculations will be described below.

Heat flux passing by the cold side of the module is absorbed by the heat sink (with liquid coolant), and it can be calculated from the following equation:

$$Q_2^* = (T_\mathrm{out} - T_\mathrm{in}) \cdot v_\mathrm{c} \cdot c_\mathrm{p}(T) \tag{2}$$

where T_out is the coolant temperature at the output of the cooler, T_in is the coolant temperature at the input of the cooler, c_p (T) is the specific heat of the liquid coolant, and v_c is the flow rate of the coolant.

The amount of heat Q_3^* converted by the module into electrical power P_el is:

$$P_{el} = Q_3^* = Q_1^* - Q_2^* \tag{3}$$

Due to the energy balance, the thermal power, Q_3^*, ought to be equal to electrical power P_el generated by the thermoelectric module. Under zero current conditions $Q_3^* = 0$, and from the energy balance we have information about energy losses before the module. When the electric current is flowing through the system, electric and thermoelectric properties of the module have to be taken into account. Peltier and Joule'a or Thomson's effects (the latter has smaller impact) cannot be omitted.

The above values of thermal powers Q_1^*, Q_2^* and electrical parameters (U_mod, I_mod, R_load) can be used to determine the essential parameters characterising thermoelectric modules. Precise characterisation of these parameters is necessary for the successful development of thermoelectric generators.

The module efficiency, η, can be calculated as a ratio of the output electric power, P_el, and the input heat by the following formula:

$$\eta = \frac{P_{el}}{Q_1^*} = \frac{Q_1^* - Q_2^*}{Q_1^*} = \frac{Q_1^* - Q_2^*}{Q_2^* + P_{el}} = \frac{Q_p^* - Q_{p0}^* - Q_j^*}{Q_{p0}^* + Q_\lambda^* - 0.5Q_j^* + P_{el}} \tag{4}$$

where Q_p^* and Q_{p0}^* are the Peltier heats exchanged in temperatures T_h and T_c. Q_λ^* is part of the heat transfer through the module under $I = 0$ A condition and Q_j^* is the Joule'a heat

$$Q_p^* = \Pi_{AB} \cdot I = T \cdot I \cdot \alpha_{AB} \tag{5}$$

Combining Eqs. 4 and 5:

$$\eta = \frac{I \cdot U_{oc} - I^2 \cdot R_{int}}{I \cdot \Pi_{AB0} + Q_\lambda^* - 0.5 \cdot I^2 \cdot R_{int} + P_{el}} \tag{6}$$

where U_{oc} is the open circuit voltage, I is the current flowing through the module and the external load, R_{int} is the internal resistance, Π_{AB}, α_{AB} are the Peltier and the Seebeck coefficients, respectively (for the TE module).

Those quantities can be obtained from the measurement data as follows. U_{oc} is the open circuit voltage on the module, when $I = 0$ *A*, [V] (Fig. 3.), R_{int} is the internal resistance, estimated form the current–voltage characteristics [Ω], $R_{int} = \Delta U / \Delta I$ (Fig. 3), Q_λ^* is the amount of heat transported by the module per time, when $I = 0$ A, [W], Π_{AB0} is the Peltier coefficient (for the module) for $T_0 = T_c = 25$°C, estimated from the differences between Q_1^*, $Q_\lambda{}^*$ and Q_j^*, for various current and temperature values [WA^{-1}].

The average heat transfer coefficient, K_c, of the module is:

$$K_c = \frac{(Q_1^* + Q_2^*)}{2 \cdot (T_h - T_c) \cdot A} \tag{7}$$

where A is the surface area of the module (top or bottom side), Q_1^* and Q_2^* which should be almost equal to Q_2^* for $I = 0$ [A], K_c is the heat transfer coefficient for $I = 0$ [A]; for different load conditions, K_c will be also a function of the electric current.

THE MEASUREMENT PROCEDURE

The TE module and measuring components of apparatus were placed in an adiabatic vacuum chamber in order to reduce the heat losses. The chamber was attached to a vacuum system, and an inert gas cylinder (Ar or N_2) provided the required atmosphere during an experiment. The TE module was placed between the heat sink and the heater. The cooler was connected to the closed-loop cooling system, which was equipped with a circulation pump controlled by the microprocessor and the precise thermostat (Julabo FP 40-MC). The thermostat could control the temperature of coolant (and heat sink, T_c) in the range of −40°C to 200°C with a step of 0.1°C and precision better than ±0.02°C. The amount of heat absorbed by the heat sink (transfer to coolant) was measured by the calibrated and certified accurate heat meter, which measures the flow rate of liquid coolant, v_c (ultrasonic Doppler method) as well as the temperatures at the inlet, T_{in}, and the outlet, T_{out}, of the heat sink by Pt500 sensors. The nominal precision of the used heat meter was better than 1%.

The temperature of the hot side, T_h, of the evaluated thermoelectric module was controlled by a thermally insulated heater, powered by an adjustable and stabilized temperature controller. The hot side temperature, T_h and the cold side temperature, T_c, of the module were measured by a *K*- type thermocouple.

Electric power, P_{el}, generated by the TE module was determined from the voltage and current measurements in an electrical circuit designed for that specific purpose. The electrical parameters of TE module as well as other electrical signals (e.g. thermocouples) were measured with an accuracy better than 0.01% by a 24-bits ADC sigma-delta converter. The electric circuit, powered by the thermoelectric module, was connected to an adjustable load resistance, R_{load}. The data collected by the system allowed us to determine the fundamental electrical parameters such as the open-circuit voltage, U_{oc}, the short circuit current, I_{sc}, and the internal resistance, R_{int}, of the module. The latter (R_{int}) was calculated from the formula:

$$R_{int} = \frac{\Delta U_{mod}}{\Delta I_{mod}} \tag{8}$$

The maximum power, P_{max} generated by the TE module and the I_{opt}, U_{opt} parameters were calculated for the load resistance $R_{opt} = R_{int}$.

Under applied measurements conditions, the maximum measurement error was lower than 3%.

The device was also equipped with a dedicated user-friendly software that enables control of all the system elements, ensures data acquisition, presentation of results in graphs, statistical analyses, and more.

CHARACTERISATION OF THERMOELECTRIC MODULES

The developed apparatus was applied in testing commercially available thermoelectric modules based on Bi_2Te_3 and Sb_2Te_3 alloys. These materials have thermoelectric figure of merit ZT of about 1 at 150°C and an average Seebeck coefficient $\alpha \sim 360$ μV/K for a semiconductor *p-n* unicouple.

The maximum operating temperature of these modules is about 200°C, but the manufacturer allows temporarily raising the temperature of the hot end, T_h up to 260°C.

The parameters of the modules provided by most producers usually relate to selected working conditions (T_c = 50°C, T_h = 175°C). However, they are insufficient to calculate such factors as power,

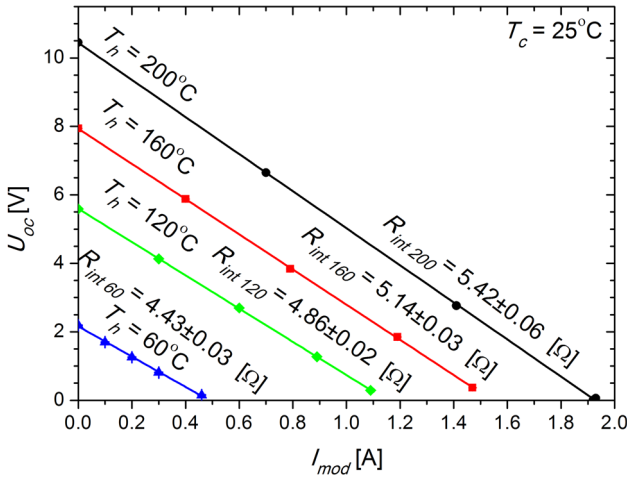

Fig. 3. Current–voltage characteristics $U = f(I)$.

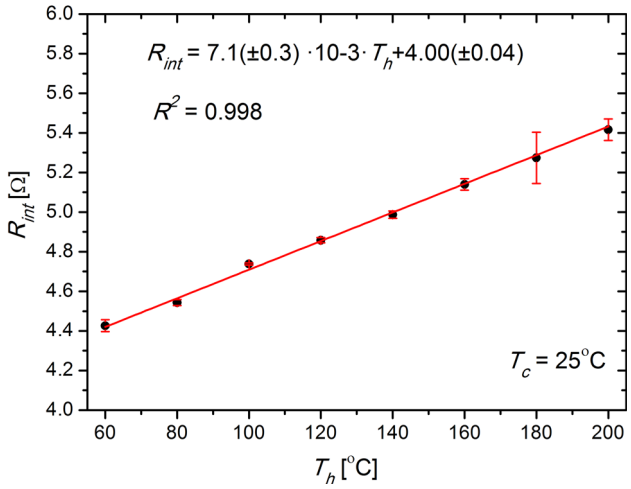

Fig. 4. Internal resistivity (R_{int}) as a function of T_h, for T_c = 25°C.

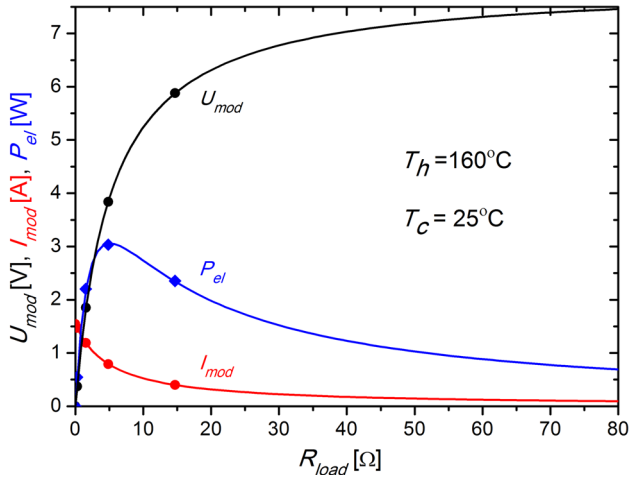

Fig. 5. Electrical power (P_{el}), load current (I_{mod}) and voltage (U_{mod}) versus electrical load resistance (R_{load}) for T_c = 25°C. Functions: $I_{mod} = U_{oc}/(R_{int} + R_{load})$, $U_{mod} = R_{load}\cdot U_{oc}/(R_{int} + R_{load})$ and $P_{el} = R_{load}\cdot(U_{oc}/(R_{int} + R_{load}))^2$.

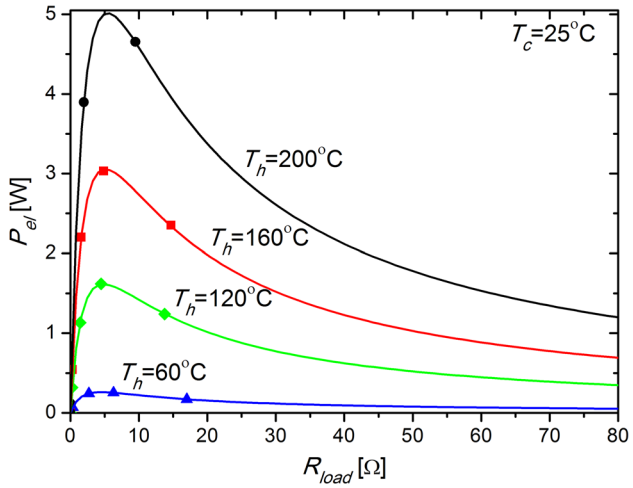

Fig. 6. Electrical power (P) versus electrical load resistance (R_{load}) for T_c = 25°C, $P_{el} = R_{load}\cdot(U_{oc}/(R_{int} + R_{load}))^2$.

efficiency, voltage and other important application parameters in a wide temperature range, as required for design and development of a generator.

The measurements were performed for several types of Bi_2Te_3 TE modules of nominal power ranging from 5 W to 7 W (at temperatures T_c = 50°C and T_h = 175°C) purchased from several manufacturers.

Results of measurements for one selected module with 241 thermoelectric *p-n* unicouples are presented in Figs. 3, 4, 5, 6, 7, 8, and 9.

Data points in current–voltage characteristics presented in Fig. 3 were averaged from ten measurements per point and for five different load currents ranging from 0 A to a maximum current value for short circuit (I_{sc}). Relations between current and voltage can be very well described by a linear function *U-f(I)*. Calculated from the line slope, internal resistances were estimated with errors lower than 1%. The internal resistances of the modules increase with the temperature, T_h = 60–200°C (T_c = 25°C), as seen Fig. 4. There are presented as data points with error bars, and the temperature range is truncated, because for T_h = 40°C the internal resistance was equal to R_{40int} = 2.99 ± 0.03 Ω. Except this first measurement, all of the calculated internal resistances fit the linear regression. This may be connected with the interaction between load source and module for small voltages and currents, regardless if the R_{40int} calculated from linear regressions had a lower value and did not fit to the trend of the $R_{int} - f(T_h)$. The data for the main cause measured operating parameters of the module (U_{mod}, P_{el}, I_{mod}) are plotted against the load resistance in Fig. 5. Measured values of each parameter are presented, along with function fits (dashed lines). The voltage on the module first increases very fast with load resistance

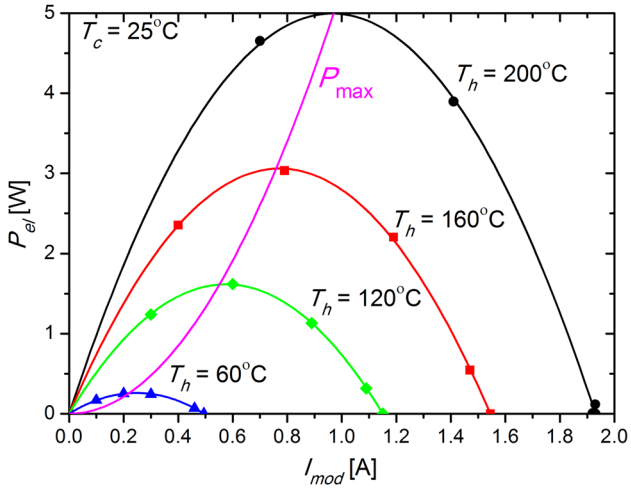

Fig. 7. Electrical power (P) versus load current (I). $P_{el} = U_{oc}\ I_{mod} - R_{int} \cdot I^2_{mod}$.

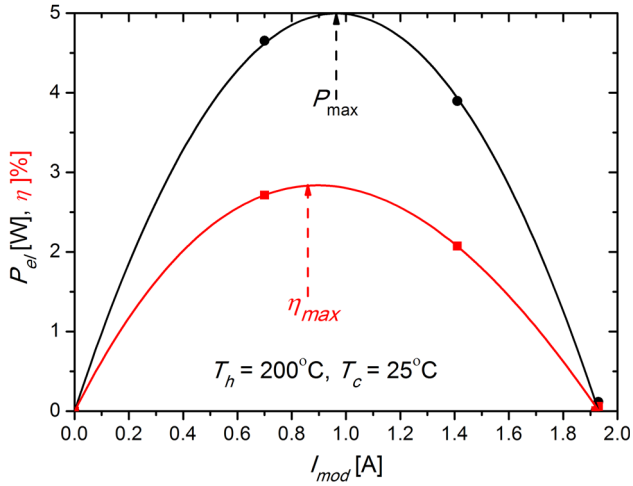

Fig. 9. Efficiency (η) and power (P_{max}) as a function of I_{mod} for T_h = 200°C and T_c = 25°C.

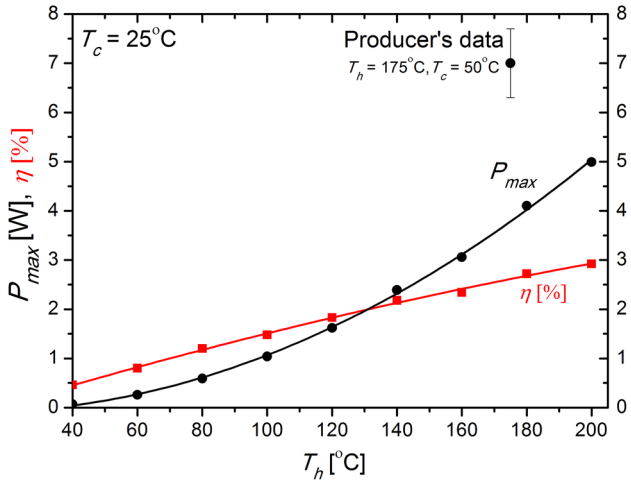

Fig. 8. Maximum efficiency (η) and maximum power (P_{max}) as a function of T_h, T_c = 25°C.

and then asymptotically approaches the open circuit voltage, U_{oc}, when R_{load} approaches infinity. The electric current is decreasing from I_{max} for short circuit to 0 when R_{load} approaches infinity. The P_{el} dependence on load resistance is more complex. First a very fast increase in power up to a maximum is observed (for optimum values of U_{mod} and I_{mod} almost equal to half of their maximum values) and then slowly decreases with increasing R_{load}. The equations for each curve are given below each figure or follow equations from the text.

Electric power (P_{el}) dependence on the load resistance for chosen T_h temperatures is presented in Fig. 6. The maximum currents are higher in higher temperatures and power dependence on current follows a parabolic function (Fig. 7). Maximum electric power for each temperature is plotted in Fig. 8, together with maximum efficiency of the module calculated from Eq. 6. To calculate this quantity, the values of U_{oc}, R_{int} are needed (one can find them analysing previously presented graphs). Furthermore, the amount of heat transferred when I_{mod} = 0 A must be known. That is the amount of heat transfer when I_{mod} = 0, and it is calculated from Eq. 2. Lastly, the Peltier coefficient was calculated from the Peltier heat equation (Q^*_{P0}). It was done by comparing Q^*_1 to the denominator of Eq. 6. The heat entering the module, Q^*_1 was calculated from Q^*_2 plus electrical power, P_{el}. Heat losses from the heater, Q^*_w, were evaluated by comparing P_h to Q^*_1 (it was assumed that in constant temperature, T_h, the losses should be constant, thus $Q^*_w = P_h - Q^*_1$ and $Q^*_1 = Q^*_2$ when I_{mod} = 0 A). In Fig. 9 calculated power and efficiency as a function of module current are plotted. One can see that the efficiency reaches the maximum value for the lower current then maximum power.

The following parameters (Table I) of the examined TE module were determined from the measurements.

The measurement module parameters for the operating module differ in our experiment from the data provided by the manufacturer. It can be explained by the possibility that the real temperature of the module is different from the measured temperatures of the hot and cold end. The real temperatures will be influenced by the thermal contact properties. In our experiment silicone pastes were used with the specific thermal conductance, λ = 0.78 W/(mK). Assuming the maximum thickness of the past fill of about 80 μm, for the maximum heat of almost 200 W, and taking into account two such thermal contacts (both sides of the module), the temperature differences is about 15°C, as outlined below. The exact value of this difference will depend on many parameters including the pressing force, roughness of the surface, the quality of the layer that is the content of entrapped gases and others. Those parameters will be considered it in

Table I. The results of the measurements and the manufacturer's data

Quantity	Measurement	Producer data
Maximum electrical power of the TE module	P_{max} = 5.0 W (T_h = 200°C and T_c = 25°C) (estimate ΔT at the module, $\Delta T_{mod} \approx 160$°C)	P_{max} = 7.0 W (for T_h = 175°C and T_c = 50°C)
Maximum efficiency	η = 3.0% (for T_h = 200°C and T_c = 25°C)	–
Heat transfer coefficient of the TE module	$K_c = 277 \pm 5$ W K^{-1} m^{-1}	–
Internal module resistance	$R_{int} = 7.1(\pm 0.3)\ 10^{-3}\ T_h + 4.00(\pm\ 0.04)\ \Omega$ (for T_h = 40…200°C and T_c = 25°C)	R_{int} = 4.5 Ω (T_h = 175°C, T_c = 50°C

our future study. For T_h = 200°C, Q_2^* = 200 W, ΔT_{mod} = 175°C, $\Delta T \approx 6.8$°C (real module temperature difference $\Delta T_{mod} \approx 175–15 = 160$°C). For T_h = 100°C, Q_2^* = 70 W, ΔT_{mod} = 75°C, $\Delta T \approx 2.4$°C (real module temperature difference $\Delta T_{mod} \approx 75–5 = 70$°C).

It is possible to measure the module material parameters more reliably using the Harman method. It was not applied in this study. Therefore, in our future work we intend to measure module material parameters for modules manufactured in our lab and analyzing all thermal properties of the whole setup that includes ceramic substrates, metal connectors, diffusion barriers and others.

SUMMARY

The constructed apparatus enables determination of the essential parameters of the TE modules in a wide range of temperatures, T_c = 5…90°C and T_h = 25…450°C. In our study the hot side temperature of the module, $T_{h\ max}$ = 200°C, was lower than the applicable temperature range of the device due to limits of the module parameters. The heat losses in the system were evaluated by comparing the heat fluxes and the electrical power. With this approach the heat fluxes for I_{mod} = 0 A must be measured. It was noticed that measurement errors were a little higher for lowest and highest T_h. In order to avoid this, in future experiments, the coolant flux will be better controlled. The maximum module efficiency was lower in our experiment than the efficiency provided by the manufacturer, but we do not know details of the measurements in which the producer value was obtained. The measurements confirmed that the developed apparatus had accuracy (better than 3%) and reproducibility of results. The equipment allows full characterisation of modules, which makes it a reliable tool for the development of thermoelectric generators.

ACKNOWLEDGEMENTS

Work presented in this paper was supported by the National Centre for Research and Development (NCBR, Poland) under the project "Innovative thermoelectric modules for energy harvesting" (project no. PBS3/A5/49/2015). This scientific work has been partially financed as a research postdoctoral project no. DEC-2014/12/S/ST8/00582 from the resources assigned for science by the National Science Centre (NCN, Poland).

OPEN ACCESS

REFERENCES

1. G.J. Snyder and E.S. Toberer, *Nat. Mater.* 7, 105 (2008).
2. D.M. Rowe, *Int J Electr. Power Energy Syst.* 1, 13 (2006).
3. H. Kawamoto, *Q. Rrev.* 30, 54 (2009).
4. K. Wojciechowski, R. Zybala, M. Schmidt, J. Merkisz, P. Fuc, and P. Lijewski, *J. Electron. Mater.* 39, 2034 (2010).
5. D.M. Rowe, *Thermoelectrics Handbook: Macro to Nano* (Boca Raton: CRC Taylor & Francis, 2005).
6. D.M. Rowe, *Handbook of Thermoelectrics, 37* (Boca Raton: CRC Press, 1995).
7. H. Böttner, D. Ebling, A. Jacquot, U. Kühn, and J. Schmidt, *J. Mater. Res.* 1044, 115 (2008).
8. R. Zybala and K.T. Wojciechowski, *AIP Conf. Proc.* 1449, 393 (2012). doi:10.1063/1.4731579.
9. V. Kosalathip, A. Dauscher, B. Lenoir, S. Migot, and T. Kumpeerapun, *Appl. Phys. A* 93, 235 (2008).
10. O. Yamashita, H. Odahara, T. Ochi, and K. Satou, *Appl. Phys. A* 94, 57 (2009).
11. M.J. Kruszewski, R. Zybala, L. Ciupinski, M. Chmielewski, B. Adamczyk-Cieslak, A. Michalski, M. Rajska, and K.J. Kurzydlowski, *J. Electron. Mater.* 45, 1369 (2016).
12. P. Nieroda, R. Zybala, and K.T. Wojciechowski, *AIP Conf. Proc.* 1449, 199 (2012). doi:10.1063/1.4731531.
13. K. Wojciechowski, M. Schmidt, J. Toboła, M. Koza, A. Olech, and R. Zybala, *J. Electron. Mater.* 39, 2053 (2010).
14. K. Wojciechowski, J. Tobola, M. Schmidt, and R. Zybala, *J. Phys. Chem. Solids* 69, 2748 (2008).
15. W. Olesinska, D. Kalinski, M. Chmielewski, R. Diduszko, and W. Wlosinski, *J. Mater. Sci-Mater. Electron.* 17, 781 (2006). doi:10.1007/s10854-006-0024-1.
16. M. Barlak, W. Olesinska, J. Piekoszewski, Z. Werner, M. Chmielewski, J. Jagielski, D. Kalinski, B. Sartowska, and K. Borkowska, *Surf. Coat. Tech.* 201, 8317 (2007).
17. L. Ciupinski, D. Siemiaszko, M. Rosinki, M. Michalski, and K.J. Kurzydlowski, *Adv. Mat. Res.* 59, 120 (2009).
18. K. Wojciechowski, R. Zybala, and R. Mania, *Microelectron. Reliab.* 51, 1198 (2011).
19. R.J. Buist and S.J. Roman, *Proceedings of 18th International Conference on Thermoelectrics* (1999), p.1.

20. M. Chmielewski and W. Weglewski, *Bull. Pol. Acad. Tech.* 61, 507 (2013). doi:10.2478/bpasts-2013-0050.
21. H. Kim, S.-G. Park, B. Jun, J. Hwang, and W. Kim, *Appl. Phys. A* 114, 1201 (2014).
22. H. Takazawa, H. Obara, Y. Okada, K. Kobayashi, T. Onishi, and T. Kajikawa, *Proceedings of 25th International Conference on Thermoelectrics ICT* (2006), p. 189.
23. H. Kaibe, I. Aoyama, M. Mukoujima, T. Kanda, S. Fujimoto, T. Kurosawa, H. Ishimabushi, K. Ishida, L. Rauscher, Y. Hata, and S. Sano, *Proceedings of 24th International Conference on Thermoelectrics ICT* (2005), p. 242.
24. L. Rauscher, S. Fujimoto, H.T. Kaibe, and S. Sano, *Meas. Sci. Technol.* 16, 1054 (2005).
25. G. Karpinski, D. Platzek, C. Stiewe, L. Rauscher, H.T. Kaibe, and E. Muller, *Proceedings of 8th European Workshop on Thermoelectrics* (2004).
26. L.I. Anatychuk and M.V. Havrylyuk, *J. Electron. Mater.* 40, 1292 (2011).
27. E. Sandos-Rosado and R. Stevens, *J. Electron. Mater.* 38, 1239 (2009).
28. A. Montecucco, J. Siviter, and A.R. Knox, *Appl. Energy* 149, 248 (2015).
29. K.T. Wojciechowski, R. Zybala, J. Leszczynski, P. Nieroda, M. Schmidt, R. Gajerski, and S. Aleksandrowa, *AIP Conf. Proc.* 1449, 467 (2012). doi:10.1063/1.4731597.
30. K. Wojciechowski, R. Zybala, and M. Schmidt, Patent PL 391503-A1, PL 217331-B1 (2012), p.1.